TISSUE ENGINEERING: Part A
Volume 14, Number 7, 2008

DOI: 10.1089/ten.tea.2007.0245

In Situ Crosslinking Elastin-Like Polypeptide Gels for Application to Articular Cartilage Repair in a Goat Osteochondral Defect Model

DANA L. NETTLES, Ph.D.,[1] KENICHI KITAOKA, M.D.,[2] NEIL A. HANSON, M.D.,[3] CHARLENE M. FLAHIFF, M.S.,[1] BRIAN A. MATA, M.D.,[4] EDWARD W. HSU, Ph.D.,[5] ASHUTOSH CHILKOTI, Ph.D.,[1] and LORI A. SETTON, Ph.D.[1,4]

ABSTRACT

The objective of this study was to evaluate an injectable, *in situ* crosslinkable elastin-like polypeptide (ELP) gel for application to cartilage matrix repair in critically sized defects in goat knees. One cylindrical, osteochondral defect in each of seven animals was filled with an aqueous solution of ELP and a biocompatible, chemical crosslinker, while the contralateral defect remained unfilled and served as an internal control. Joints were sacrificed at 3 ($n = 3$) or 6 ($n = 4$) months for MRI, histological, and gross evaluation of features of biomaterial performance, including integration, cellular infiltration, surrounding matrix quality, and new matrix in the defect. At 3 months, ELP-filled defects scored significantly higher for integration by histological and gross grading compared to unfilled defects. ELP did not impede cell infiltration but appeared to be partly degraded. At 6 months, new matrix in unfilled defects outpaced that in ELP-filled defects and scored significantly better for MRI evidence of adverse changes, as well as integration and proteoglycan-containing matrix via gross and histological grading. The ELP-crosslinker solution was easily delivered and formed stable, well-integrated gels that supported cell infiltration and matrix synthesis; however, rapid degradation suggests that ELP formulation modifications should be optimized for longer-term benefits in cartilage repair applications.

INTRODUCTION

ARTICULAR CARTILAGE IS a hyaline cartilage material lining the bones in diarthrodial joints that contributes to load distribution, energy dissipation, and lubrication.[1–3] Articular cartilage is avascular, alymphatic, and aneural,[1,4] such that partial thickness injuries have little capacity for intrinsic regeneration. Even in full thickness injuries where fibrocartilaginous tissue forms from the diffusion of a fibrin clot into the defect, regeneration is generally nonfunctional and fails long-term.[5–7]

With autologous chondrocyte transplantation (ACI), a patient's own cells are expanded *ex vivo* and reimplanted in a cartilage defect under an autologous periosteal flap.[8,9] In applications termed second- and third-generation ACI procedures, various biological or polymer membranes or scaffolds have been used *in lieu* of the periosteal flap. This approach alleviates the need to harvest and suture

[1]Department of Biomedical Engineering, Duke University, Durham, North Carolina.
[2]Department of Orthopaedic Surgery, Kochi Medical School, Kochi, Japan.
[3]Department of Anesthesiology, Duke University Medical Center, Durham, North Carolina.
[4]Department of Surgery, Duke University Medical Center, Durham, North Carolina.
[5]Department of Bioengineering, University of Utah, Salt Lake City, Utah.
This work was presented at the Sixth Symposium of the International Cartilage Repair Society in January 2006.

autologous periosteum and provides scaffolds that promote cell retention, thereby simplifying the surgical procedure and possibly reducing hypertrophy often associated with periosteal flaps.[10,11]

Injectable, *in situ* forming scaffolds may offer some advantages over existing methods of regenerating focal defects, because their liquid-like properties prior to injection allow mixing with cells or other factors, and permit complete filling of irregularly shaped defects, which could enhance integration of newly generated tissue with the existing native tissue. Many hydrogel materials are capable of *in situ* crosslinking and have been evaluated for the potential to promote cartilage matrix regeneration, including poly (ethyleneoxide),[12–14] poly(*N*-isopropylacrylamide),[15] fibrin,[16,17] hyaluronic acid,[18] and chitosan.[19]

Elastin-like polypeptides (ELPs) are genetically engineered proteins constructed from a portion of the native elastin sequence (V–P–G–X–G),[20] where X may be any amino acid except proline.[21] ELPs are attractive for tissue engineering applications because their physical properties can be precisely controlled at the gene level through control of the molecular weight of the polypeptide, as well as the degree of crosslinking by specifying the number and location of crosslinking sites.[22–28] Further, ELPs are environmentally responsive, as they exhibit an inverse phase transition at a temperature (T_t), above which they undergo hydrophobic collapse and form a gel-like "aggregated" mass, which enables the synthesis of ELPs that undergo *in situ* gelling, and may possess a range of properties.[21,23,27,29,30] Physicochemical properties are dependent on the genetic sequence of the ELP, which dictates transition temperature, crosslink density, and responsiveness to other environmental factors, including sensitivity to changes in pH, as well as concentrations of solute and solvent concentrations. ELPs have also been shown not to elicit an immune response when injected subcutaneously.[31]

We have previously shown uncrosslinked ELPs to support chondrogenesis for primary chondrocytes[29] and chondrocyte precursor cells *in vitro*.[32] We have also shown that ELPs retain this ability when they are enzymatically crosslinked.[24] However, these uncrosslinked and enzymatically crosslinked ELPs were not suitable for implantation in a cartilage defect because their mechanical properties were inadequate for contributing to load support. In this study, ELP formulations were designed that contain lysine (K),[23,27] so they could be chemically crosslinked with an amine-reactive crosslinker (β-[Tris(hydroxymethyl)phosphino] propionic acid [betaine]), THPP. The byproducts of this reaction are water and chemically stable aminomethylphosphines and so are biocompatible for crosslinking with cells.[23] ELPs crosslinked with this system result in gels having compressive and shear stiffness on the order of 10–50 kPa, and 2–3 orders of magnitude greater than those reported for uncrosslinked ELP,[23,29,33] and scaffolds can be formed in clinically relevant time scales (<5 min).[23] The objective of this study was to evaluate an injectable THPP-crosslinkable formulation of ELP for defect filling in critically sized goat osteochondral defect model. Full-thickness defects filled with the *in situ* crosslinkable ELP were evaluated after 3 and 6 months by grading of MRI, histological, and gross appearance to assess essential features of biomaterial performance, including integration, cellular infiltration, surrounding matrix quality, and new matrix in the defect.

MATERIALS AND METHODS

Expression and purification of elastin-like polypeptides

Genes encoding ELPs of amino acid sequence VPG<u>K</u>G(VPG<u>V</u>G)$_6$-224, termed [KV$_6$-224] (MW = 93.4 kDa), were expressed in *Escherichia coli* BLR(DE3) (Novagen, Madison, WI) as previously described (Terrific Broth™ Dry Growth Media [MoBio Laboratories, Carlsbad, CA], 100 μg/mL of ampicillin).[27] Expressed proteins were purified from cell lysates using inverse transition cycling (ITC),[34] followed by suspension in 25 mM HEPES-buffered saline and sterile filtration using a low-protein binding 0.22 μm syringe filter (Millex-GV PVDF; Millipore, Billerica, MA). Purified ELPs were concentrated to 200 mg/mL and stored at −80°C until further use.

Preparation of crosslinker

A trifunctional, water-soluble, amine-reactive crosslinker (β-[Tris(hydroxymethyl)phosphino]propionic acid [betaine]) (THPP; Pierce Biotechnology, Rockford, IL) was solubilized in 200 μL of 25 mM HEPES-buffered saline to a final concentration of 250 mg/mL. Aliquots of this solution were stored at −80°C until further use.

Creation of osteochondral defects

All procedures were performed in accordance with the Duke University Institutional Animal Care and Use Committee. Eight Nubian goats (80–130 lb (36.29–58.97 kg); four female and four males) underwent surgery to create 6 mm diameter×4 mm deep osteochondral defects in the medial femoral condyles of both knees. This dimension was chosen in this model based on prior research by Jackson *et al.*[35] showing that bone–cartilage defects of this dimension do not spontaneously heal. In this technique, the cartilage surface was exposed via a medial parapatellar incision, and a 6 mm diameter Forstner drill bit was used to create the defects. In each animal, one defect was filled with a solution (approximately 150 μL) of 200 mg/mL ELP [KV$_6$-224] and THPP at a 1:1.7 ratio of crosslinking sites via an 18-gauge syringe needle. The contralateral defect in each goat was left unfilled as an internal control (Fig. 1). Control and ELP-filled knees were randomized amongst the

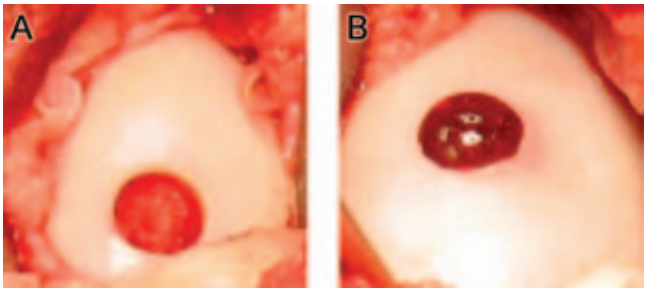

FIG. 1. Representative defects left unfilled (**A**) and ELP-filled (**B**) at the time of surgery (time zero).

animals. A pilot study was conducted to determine the ability of a crosslinked ELP to remain in the defect after short periods of joint loading. This study demonstrated that ELP was still present at 7 days after surgery, and the animals showed no ill signs due to the surgical method. Therefore, in this study, three animals were sacrificed 3 months postoperatively, and four animals were sacrificed 6 months postoperatively. One animal died from aspiration immediately postoperatively; joints were harvested from this animal for evaluation of biomaterial filling and defect creation. Animals recovered in the vivarium for 2 weeks without any weight-bearing restrictions before returning to pasture until sacrifice.

MRI evaluation

After sacrifice, joints were wrapped in saline-soaked gauze and parafilm, and placed in airtight bags for imaging. MRI imaging was performed on a 7.1 T horizontal-bore instrument (Oxford Magnet, Oxfordshire, United Kingdom) to acquire 2D coronal images of the goat knee joints (256×256 matrix size, 6×6 cm FOV, 1.5 mm slice thickness, TR = 500 ms, TE = minimum, flip angle = 60°, eight averages). Images were graded by three blinded readers according to a scale with features of signal, defect fill, and bone edema (adapted from Henderson *et al.*[36]) as well as features of surface integrity and contour and cartilage thickness (adapted from Marlovits *et al.*[37]). The scale was adapted to allow for representation of features from both of the referenced grading schemes used previously, and a four-category ranking was used for each feature for consistency across schemes (0–3, 3 = nondegenerate cartilage). Graders included an orthopaedic surgeon and two cartilage researchers. Graders were trained in each scoring system before grading was performed.

Gross evaluation

Following MRI, joints were opened and evaluated for gross appearance. Each joint was graded by three blinded readers according to a semiquantitative grading scheme adapted from the ICRS Cartilage Injury Evaluation Package to include features of defect filling (vertical/horizontal fill, fill pattern, and integration with native tissue), defect consistency, and surrounding articular surface. Adaptations were made to separately grade features of integration and defect consistency, as short-term biomaterial integration was a performance feature of importance. Each category was graded on a 0–3 or 0–4 point scale, where 3 or 4 represents healthy cartilage.

Histological assessment

Following gross evaluation of joints, cartilage–bone blocks encompassing the entire diameter of the defect were prepared for histology. Blocks were decalcified in saturated EDTA, embedded in paraffin, and 8 μm sections were stained with Masson's trichrome, hematoxylin and eosin, and Safranin-O, along with immunostaining for types I (C2456, Sigma, St. Louis, MO) and II (II-II6B3; DSHB, Iowa City, IA) collagen. Sections were graded by three blinded readers according to a semiquantitative scale adapted from two schemes to incorporate features of integration or "bonding," total collagen, bone–cartilage architecture representing "structure" (from Odriscoll *et al.*[38]) or "subchondral bone" (from the ICRS Visual Histological Assessment[39]), proteoglycan staining, and types I and II collagen staining (adapted from Matrix category of ICRS to separate scoring for each collagen). Here, as for MRI and gross grading scales, two scales were combined to obtain

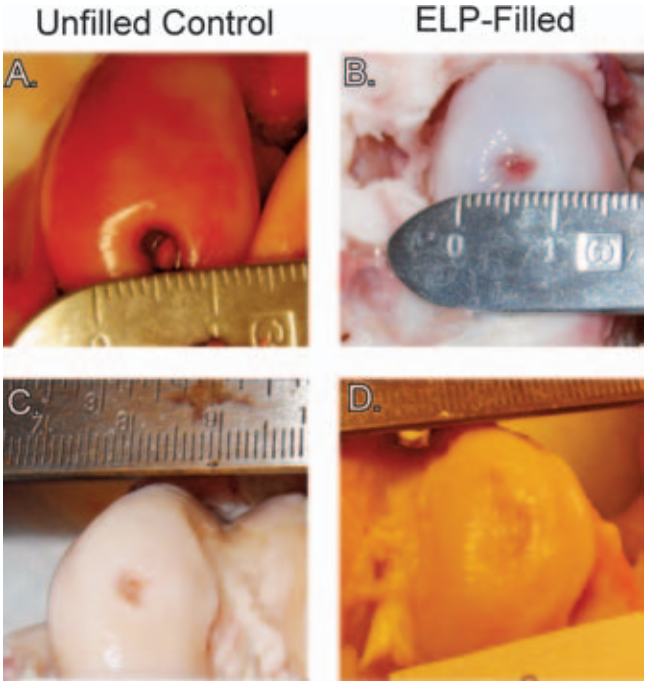

FIG. 2. Images of representative (**A, C**) unfilled control and (**B, D**) ELP-filled defects at 3 (**A, B**) or 6 (**C, D**) months. Defects shown for a given time point are from one animal. Note bony tissue forming in the center of the 3-month unfilled control defect, and in both defects at 6 months.

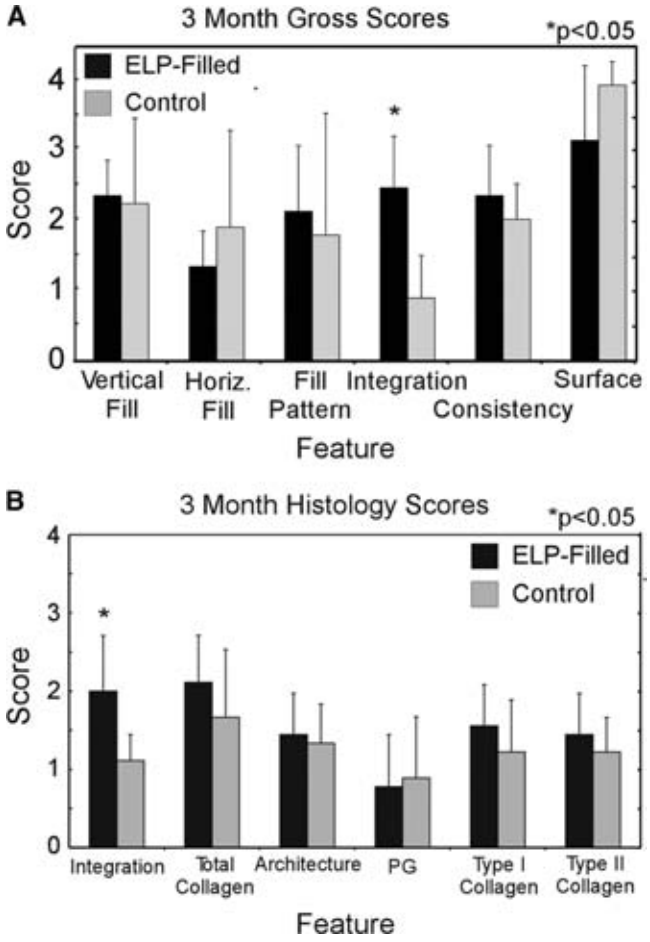

FIG. 3. Semiquantitative scores for (**A**) gross appearance (scale: 0–3) and (**B**) histology (scale: 0–3) for 3-month animals ($n = 3$). Higher scores for type I collagen reflect a lack of staining, while higher scores for type II collagen reflect abundant staining. Values represent the mean ± the standard deviation.

the maximum information on all features for biomaterial performance. Each section was graded on a 0–3 point scale for each feature, where 3 represents a section from a healthy joint. For the feature of type I collagen, higher scores reflect a lack of staining, while higher scores for type II collagen reflect abundant staining, as would be consistent with healthy cartilage.

Statistics

Statistical analysis of MRI, gross, and histological grades were performed at each time point using a paired *t*-test to test for differences between the ELP-filled and control defects for each feature in a given scale. Scores were averaged across graders before statistical analyses were performed. Statistical significance was determined at a *p*-value of 0.05. Values are presented as the mean ± the standard deviation of the mean score for a given time point. Statistical analyses were performed using StatView software (SAS Institute, Cary, NC).

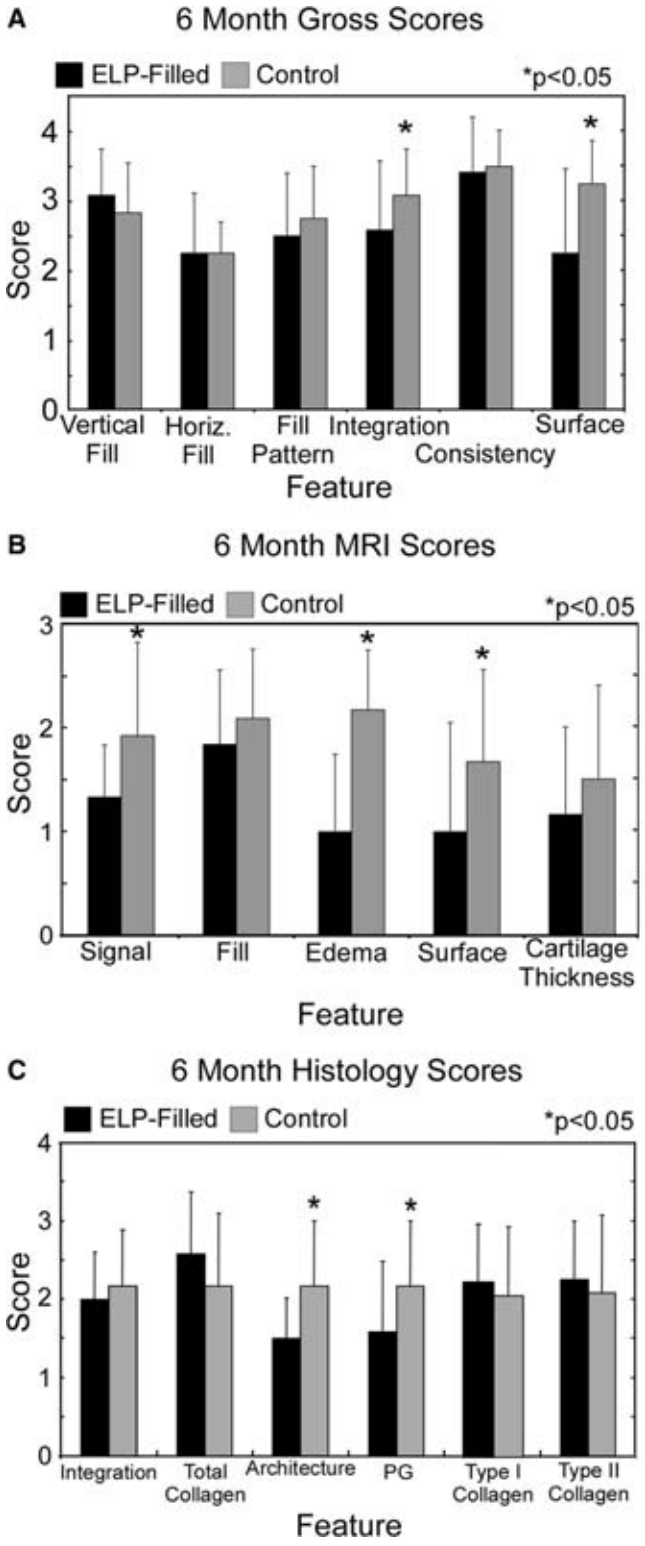

FIG. 4. Semiquantitative scores for (**A**) gross appearance (scale: 0–3), (**B**) MR images (scale: 0–3), and (**C**) histology (scale: 0–3) for 6-month animals ($n = 4$). For the feature type I collagen, higher scores reflect a lack of staining, while higher scores for type II collagen reflect abundant staining. Values represent the mean ± the standard deviation.

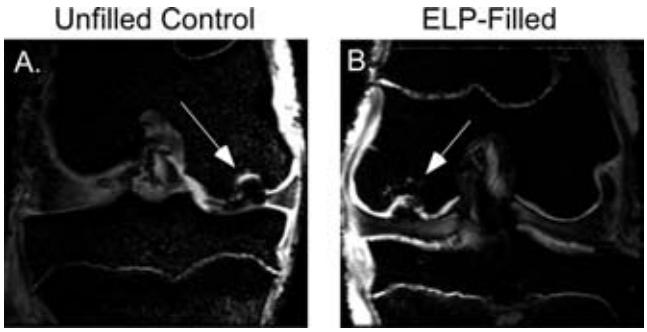

FIG. 5. Representative 3-month MR images in which defects can be clearly located for both (**A**) unfilled control and (**B**) ELP-filled defects. Defects are marked by arrows.

RESULTS

Gross appearance

At 3 months, defects were clearly evident in both ELP-filled and control defects but had mostly decreased in size from the original 6 mm diameter to 3–5 mm (Fig. 2). Two of three unfilled control defects contained bony tissue in the center (Fig. 2A), with one defect being almost entirely filled with this tissue. There was clear demarcation between the tissue filling these defects and the native articular cartilage surface. Similar observations were noted at 6 months (Fig. 2C and D), and there was no observable evidence of ELP material remaining in the defects, suggesting that the material had been degraded by this time point.

Scoring of gross appearance revealed that ELP-filled defects scored higher than control defects for integration ($p < 0.05$, Fig. 3A). By 6 months, unfilled defects scored significantly higher for integration and surrounding articular surface compared to ELP-filled defects ($p < 0.05$, Fig. 4A). Differences in other features were not observed.

MRI analysis

Joints from two 3-month animals were imaged via MRI; joints from the third animal were too large to image in this scanner. Defects were evident on MRI at 3 months post-surgery for both ELP-filled and control joints and contained large areas of increased T2-weighted signal in the subchondral bone, as well as evidence of interrupted articular cartilage surfaces (Fig. 5). Marked bone edema was evident in both control and ELP-filled defects. Because joints from only two of the three animals were imaged, statistical analysis of differences was not performed. While it is difficult to make any conclusions based on only two animals, trends at 3 months suggested that ELP filled defects scored higher for degree of filling, surface integrity and contour, and cartilage thickness, and lower for signal and edema.

By 6 months, MRI images of control defects scored significantly better for signal, edema, and surface integrity versus ELP-filled defects ($p < 0.05$, Fig. 4B). MR images also showed interanimal variability and intraanimal similarity in healing tendencies, suggesting the importance of intraanimal controls when feasible.

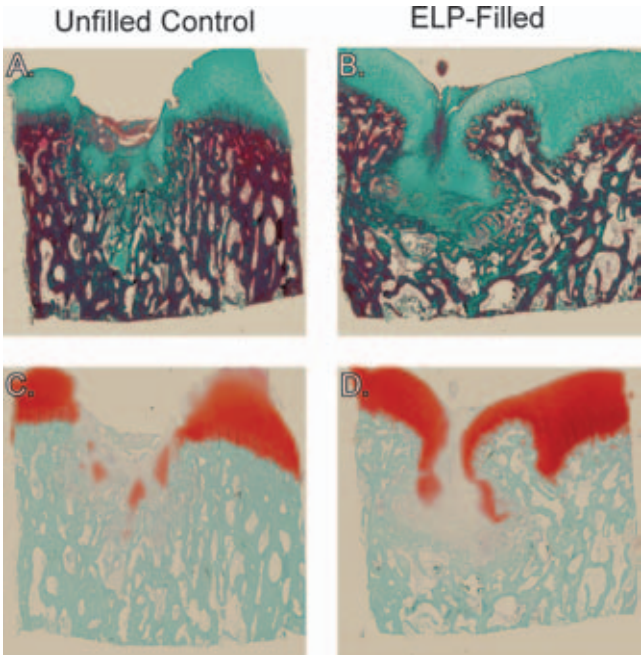

FIG. 6. Representative histological images of (**A, C**) an unfilled control defect and (**B, D**) an ELP-filled defect from a 3-month animal stained with Masson's trichrome (green, **A** and **B**) for collagen and Safranin-O (red, **C** and **D**) for proteoglycans. Note the collapse of the subchondral bone for both cases, but better integration of newly formed tissue with native tissue in the ELP-filled images.

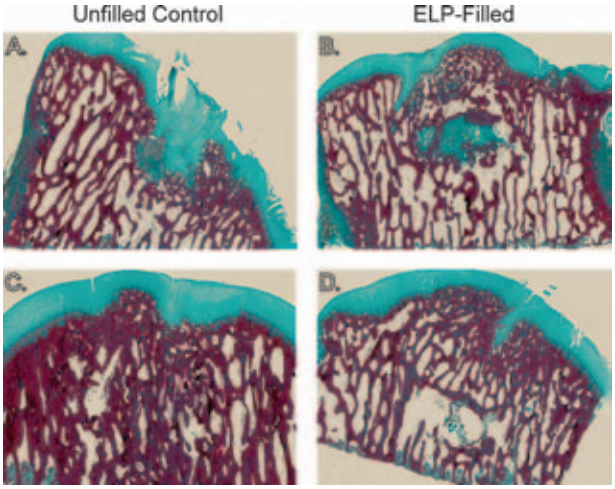

FIG. 7. Representative histological sections from (**A, C**) unfilled control and (**B, D**) ELP-filled defects from two 6-month animals stained with Masson's trichrome for collagen. (**A**) and (**B**) are sections from one animal, while (**C**) and (**D**) are sections from another animal. The variable healing between animals was also observed upon gross examination.

Histological analysis

Semiquantitative grading of 3-month histological images revealed that ELP-filled defects showed significantly better integration than control defects ($p < 0.05$, power $= 0.20$, Fig. 3B), consistent with findings from gross evaluation. Grading of histological sections at 6 months revealed that ELP-filled defects scored significantly lower for architecture and proteoglycan ($p < 0.05$, Fig. 4C). On average, differences noted between joints via histological grading did not exceed one grading point for each feature.

At 3 months, histological analysis confirmed observations made during gross evaluation. As anticipated, the unfilled control defects exhibited substantial collapse and remodeling of the underlying subchondral bone that is consistent with the work of Jackson *et al*.[35] Indeed, this model was chosen for the property that the unfilled osteochondral defects do not spontaneously heal as was observed (Fig. 6A and C). The ELP-filled defects exhibited a similar collapse of the underlying subchondral bone with evidence of cartilaginous matrix filling in the collapsed region; nevertheless, this finding suggests that the defect created a hostile environment for ELP assisted repair (Fig. 6B and D). There was no restoration of the tidemark in control or ELP-filled defects, and all samples were characterized by reduced Safranin-O staining in the superficial zone of the adjacent tissue and in the new tissue filling the defects (Fig. 6C and D).

By 6 months, tidemark restoration was only detectable in defects in one animal and was evident in both control and ELP-filled defects in this one animal (Fig. 7C and D). Areas of incomplete bony tissue remodeling were evident in all ELP-filled defects (Fig. 7B and D) and in two of four control defects. With the exception of one animal, both ELP-filled and control defects stained positively for type II collagen in regenerated cartilaginous tissue and stained bright red with Safranin-O for proteoglycans in a similar pattern.

DISCUSSION

This study evaluated an injectable and *in situ* crosslinkable ELP gel for biomaterial performance in a cartilage defect–filling application. Critically sized osteochondral defects in a goat femoral condyle were easily filled with a cell-free solution of ELP/THPP that was allowed to crosslink for 5 min. Joints were harvested after 3 or 6 months and evaluated by grading of MRI, histological, and gross appearance to assess essential features of ELP performance, including integration, cellular infiltration, surrounding matrix quality, and matrix regeneration in the defect. At 3 months after filling, ELP-filled defects scored higher than control defects for biomaterial integration as determined by gross and histological grading. By 6 months, however, ELP-filled defects were associated with poorer repair scores or scores for most features that were not different from controls. The very small number of animals evaluated here precluded an ability to form conclusions about ELP performance with any meaningful statistical power. Nevertheless, some important features of ELP performance were observed including an ability of the crosslinked ELP to support cell infiltration, and to be resorbed from the defect site. As ELP was delivered completely cell-free in this study, the presumed source of infiltrating cells was bone marrow space or adjacent synovium. We have previously shown that undifferentiated cells synthesize cartilaginous matrix components when cultured in ELPs,[32] suggesting that the crosslinked ELP in the defects would not only contribute to an ability to sustain load, but would have the potential to promote chondrocytic differentiation of infiltrating cells. However, the addition of cells to the ELP at the time of injection may be desirable in future studies to potentially accelerate or improve healing.

MR images were used in this study as a noninvasive tool for evaluating the defects *in situ*. In general, defects were easily visualized at 3 and 6 months on MRI for ELP-filled and control groups. A recurring feature in both control and ELP-filled defects was the presence of bony edema at both time points. This phenomenon has been routinely observed in conjunction with other cartilage repair procedures, including microfracture, osteochondral grafting, and autologous chondrocyte implantation, and is thought to be attributed to osseous remodeling and/or fibrovascular tissue.[40] Bone edema is reported to be most common in the first month of repair but has been observed to persist in even asymptomatic patients for up to 1 year.[40,41] This edema interfered with clear visualization of the cartilage–bone interface, calling into question the utility of gradient echo MRI data for that purpose.

Histological sections revealed the degree of collagen and proteoglycan matrix accumulation in the filled and unfilled defects, as well as remodeling of the proper joint structure. At 3 months, there was little difference in the histological appearance of control and ELP-filled defects, with evidence of large areas adjacent to bone collapse that remained empty or contained tissue that did not resemble native tissue. The ELP hydrogel was largely absent from the defect by 3 months, however, likely related to proteolytically mediated degradation of the ELP.[42] This may explain why repair in control defects outpaced ELP-filled defects at the 6-month time point. Because ELPs are genetically engineered, the degradation, crosslink density, transition temperature, and other properties of these gels are parameters that may be altered in a well-controlled manner to achieve a slower degradation rate.

There was a noticeable difference in gross appearance of all ELP-filled and unfilled control defects between the 3- and 6-month time points, with all 6-month defects being of smaller diameter and shallower depth than the 3-month defects. Nevertheless, complete or nearly complete healing was not observed in any group of animals, reinforcing the severity of the animal model studied here. The defect size and type chosen in this study (6 mm diameter$\times$4 mm

deep)[35] is not physiologically representative of most human pathology, and so may not be optimal for evaluating clinical relevance to the human case. The goal of this study, however, was to evaluate key performance features of the ELP gels and to minimize contributions to repair caused by spontaneous healing. To replicate the relevant clinical condition and to avoid challenges in placing ELP in the bony compartment, future studies of a purely chondral lesion would be desired.

In conclusion, elastin-like polypeptide gels were investigated as defect-filling materials for cartilage repair in a large osteochondral defect. Crosslinkable ELP was easily injected into critically sized defects and formed stable gels within 5 min. The presence of the crosslinked gel did not impede cell infiltration, and appeared to promote better integration at early time points. Tissue filling the defects at both late and early time points contained markers of hyaline cartilage, type II collagen, and proteoglycan, although a rapid degradation of the crosslinked hydrogel may have inhibited long-term survival of the 3D scaffold, resulting in long-term repair that largely resembled that in unfilled defects. While degradation of the hydrogel has been shown to be favorable for new matrix synthesis and accumulation,[43] preservation of the biomaterial may be desirable over longer-time periods than shown here. Based on the outcomes of this study, the addition of cells or the modification of the degradation behavior, as well as other ELP features, may be necessary to afford long-term benefits of this ELP for cartilage defect-filling applications.

ACKNOWLEDGMENTS

This work was supported by NIH EB002263. The authors thank Steve Johnson and Ryan Maker for assisting with animal surgeries, and Dong Woo Lim for assisting with crosslinking chemistry.

REFERENCES

1. Buckwalter, J.A. Articular cartilage. Instruct Course Lect **32,** 349, 1983.
2. Buckwalter, J.A., and Mankin, H.J. Articular cartilage. I. Tissue design and chondrocyte–matrix interactions. J Bone Joint Surg-Am **79A,** 600, 1997.
3. Muir, H. The chondrocyte, architect of cartilage—biomechanics, structure, function and molecular-biology of cartilage matrix macromolecules. Bioessays **17,** 1039, 1995.
4. Huber, M., Trattnig, S., and Lintner, F. Anatomy, biochemistry, and physiology of articular cartilage. Invest Radiol **35,** 573, 2000.
5. Buckwalter, J.A. Articular cartilage injuries. Clin Orthop Rel Res Issue 402, 21, 2002.
6. Buckwalter, J.A., and Mankin, H.J. Articular cartilage. II. Degeneration and osteoarthrosis, repair, regeneration, and transplantation. J Bone Joint Surg-Am **79A,** 612, 1997.
7. Hunziker, E.B. Articular cartilage repair: are the intrinsic biological constraints undermining this process insuperable? Osteoarthritis Cartilage **7,** 15, 1999.
8. Brittberg, M., Nilsson, A., Lindahl, A., Ohlsson, C., and Peterson, L. Rabbit articular cartilage defects treated with autologous cultured chondrocytes. Clin Orthop Rel Res **326,** 270, 1996.
9. Grande, D.A., Pitman, M.I., Peterson, L., Menche, D., and Klein, M. The repair of experimentally produced defects in rabbit articular-cartilage by autologous chondrocyte transplantation. J Orthop Res **7,** 208, 1989.
10. Brittberg, M., Peterson, L., Sjogren-Jansson, E., Tallheden, T., and Lindahl, A. Articular cartilage engineering with autologous chondrocyte transplantation—a review of recent developments. J Bone Joint Surg-Am **85A,** 109, 2003.
11. Marlovits, S., Zeller, P., Singer, P., Resinger, C., and Vecsei, V. Cartilage repair: generations of autologous chondrocyte transplantation. Eur J Radiol **57,** 24, 2006.
12. Elisseeff, J., Anseth, K., Sims, D., McIntosh, W., Randolph, M., Yaremchuk, M., and Langer, R. Transdermal photopolymerization of poly(ethylene oxide)-based injectable hydrogels for tissue-engineered cartilage. Plast Reconstr Surg **104,** 1014, 1999.
13. Saim, A.B., Cao, Y.L., Weng, Y.L., Chang, C.N., Vacanti, M.A., Vacanti, C.A., and Eavey, R.D. Engineering autogenous cartilage in the shape of a helix using an injectable hydrogel scaffold. Laryngoscope **110,** 1694, 2000.
14. Sims, C.D., Butler, P.E.M., Casanova, R., Lee, B.T., Randolph, M.A., Lee, W.P.A., Vacanti, C.A., and Yaremchuk, M.J. Injectable cartilage using polyethylene oxide polymer substrates. Plast Reconstr Surg **98,** 843, 1996.
15. Stile, R.A., Burghardt, W.R., and Healy, K.E. Synthesis and characterization of injectable poly(*N*-isopropylacrylamide)-based hydrogels that support tissue formation *in vitro*. Macromolecules **32,** 7370, 1999.
16. Passaretti, D., Silverman, R.P., Huang, W., Kirchhoff, C.H., Ashiku, S., Randolph, M.A., and Yaremchuk, M.J. Cultured chondrocytes produce injectable tissue-engineered cartilage in hydrogel polymer. Tissue Eng **7,** 805, 2001.
17. Silverman, R.P., Passaretti, D., Huang, W., Randolph, M.A., and Yaremchuk, M. Injectable tissue-engineered cartilage using a fibrin glue polymer. Plast Reconstr Surg **103,** 1809, 1999.
18. Nettles, D.L., Vail, T.P., Morgan, M.T., Grinstaff, M.W., and Setton, L.A. Photocrosslinkable hyaluronan as a scaffold for articular cartilage repair. Ann Biomed Eng **32,** 391, 2004.
19. Hoemann, C.D., Sun, J., Legare, A., McKee, M.D., and Buschmann, M.D. Tissue engineering of cartilage using an injectable and adhesive chitosan-based cell-delivery vehicle. Osteoarthritis Cartilage **13,** 318, 2005.
20. Sandberg, L.B., Soskel, N.T., and Leslie, J.G. Elastin structure, biosynthesis, and relation to disease states. N Engl J Med **304,** 566, 1981.
21. Urry, D.W. Free-energy transduction in polypeptides and proteins based on inverse temperature transitions. Prog Biophys Mol Biol **57,** 23, 1992.
22. Lee, J., Macosko, C.W., and Urry, D.W. Elastomeric polypentapeptides cross-linked into matrixes and fibers. Biomacromolecules **2,** 170, 2001.

23. Lim, D.W., Nettles, D.L., Setton, L.A., and Chilkoti, A. Rapid crosslinking of elastin-like polypeptides with hydroxymethylphosphines in aqueous solution. Biomacromolecules **8,** 1463, 2007.
24. McHale, M.K., Setton, L.A., and Chilkoti, A. Synthesis and *in vitro* evaluation of enzymatically cross-linked elastin-like polypeptide gels for cartilaginous tissue repair. Tissue Eng **11,** 1768, 2005.
25. Nagapudi, K., Brinkman, W.T., Leisen, J.E., Huang, L., McMillan, R.A., Apkarian, R.P., Conticello, V.P., and Chaikof, E.L. Photomediated solid-state cross-linking of an elastin-mimetic recombinant protein polymer. Macromolecules **35,** 1730, 2002.
26. Nowatzki, P.J., and Tirrell, D.A. Physical properties of artificial extracellular matrix protein films prepared by isocyanate crosslinking. Biomaterials **25,** 1261, 2004.
27. Trabbic-Carlson, K., Setton, L.A., and Chilkoti, A. Swelling and mechanical behaviors of chemically cross-linked hydrogels of elastin-like polypeptides. Biomacromolecules **4,** 572, 2003.
28. Urry, D.W., Pattanaik, A., Xu, J., Woods, T.C., McPherson, D.T., and Parker, T.M. Elastic protein-based polymers in soft tissue augmentation and generation. J Biomater Sci-Polym Ed **9,** 1015, 1998.
29. Betre, H., Setton, L.A., Meyer, D.E., and Chilkoti, A. Characterization of a genetically engineered elastin-like polypeptide for cartilaginous tissue repair. Biomacromolecules **3,** 910, 2002.
30. Meyer, D.E., and Chilkoti, A. Genetically encoded synthesis of protein-based polymers with precisely specified molecular weight and sequence by recursive directional ligation: examples from the elastin-like polypeptide system. Biomacromolecules **3,** 357, 2002.
31. Urry, D.W., Parker, T.M., Reid, M.C., and Gowda, D.C. Biocompatibility of the bioelastic materials, poly(GVGVP) and its gamma-irradiation cross-linked matrix—summary of generic biological test-results. J Bioactive Comp Polym **6,** 263, 1991.
32. Betre, H., Ong, S.R., Guilak, F., Chilkoti, A., Fermor, B., and Setton, L.A. Chondrocytic differentiation of human adipose-derived adult stem cells in elastin-like polypeptide. Biomaterials **27,** 91, 2006.
33. Hanson, N.A., Nettles, D.L., Vail, T.P., Lim, D.W., Chilkoti, A., and Setton, L.A. Mechanical characterization and *in vitro* chondrogenic evaluation of chemically crosslinked elastin-like polypeptide hydrogels. Trans Orthop Res Soc **31,** Paper #807, 2006.
34. Meyer, D.E., and Chilkoti, A. Purification of recombinant proteins by fusion with thermally responsive polypeptides. Nat Biotechnol **17,** 1112, 1999.
35. Jackson, D.W., Lalor, P.A., Aberman, H.M., and Simon, T.M. Spontaneous repair of full-thickness defects of articular cartilage in a goat model—a preliminary study. J Bone Joint Surg-Am **83A,** 53, 2001.
36. Henderson, I.J.P., Tuy, B., Connell, D., Oakes, B., and Hettwer, W.H. Prospective clinical study of autologous chondrocyte implantation and correlation with MRI at three and 12 months. J Bone Joint Surg-Br **85B,** 1060, 2003.
37. Marlovits, S., Striessnig, G., Resinger, C.T., Aldrian, S.M., Vecsei, V., Imhof, H., and Trattnig, S. Definition of pertinent parameters for the evaluation of articular cartilage repair tissue with high-resolution magnetic resonance imaging. Eur J Radiol **52,** 310, 2004.
38. Odriscoll, S.W., Keeley, F.W., and Salter, R.B. Durability of regenerated articular-cartilage produced by free autogenous periosteal grafts in major full-thickness defects in joint surfaces under the influence of continuous passive motion—a follow-up report at one year. J Bone Joint Surg-Am **70A,** 595, 1988.
39. Mainil-Varlet, P., Aigner, T., Brittberg, M., Bullough, P., Hollander, A., Hunziker, E., Kandel, R., Nehrer, S., Pritzker, K., Roberts, S., and Stauffer, E. Histological assessment of cartilage repair—a report by the histology endpoint committee of the international cartilage repair society (ICRS). J Bone Joint Surg-Am **85A,** 45, 2003.
40. Recht, M., White, L.M., Winalski, C.S., Miniaci, A., Minas, T., and Parker, R.D. MR imaging of cartilage repair procedures. Skeletal Radiol **32,** 185, 2003.
41. Verstraete, K.L., Almqvist, F., Verdonk, P., Vanderschueren, G., Huysse, W., Verdonk, R., and Verbrugge, G. Magnetic resonance imaging of cartilage and cartilage repair. Clin Radiol **59,** 674, 2004.
42. Ong, S.R., Carlson, K.T., Nettles, D.L., Lim, D.W., Chilkoti, A., and Setton, L.A. Epitope tagging for tracking elastin-like polypeptides. Biomaterials **27,** 1930, 2006.
43. Bryant, S.J., Bender, R.J., Durand, K.L., and Anseth, K.S. Encapsulating chondrocytes in degrading PEG hydrogels with high modulus: engineering gel structural changes to facilitate cartilaginous tissue production. Biotechnol Bioeng **86,** 747, 2004.

Address reprint requests to:
Lori A. Setton, Ph.D.
Department of Biomedical Engineering
Duke University
136 Hudson Hall, Box 90281, Science Drive
Durham, NC 27708

E-mail: setton@duke.edu

Received: August 4, 2007
Accepted: January 10, 2008